

# Diffuse Source Mapping with MAXI

Emi Miyata,<sup>1</sup> and MAXI team

<sup>1</sup> Department of Earth & Space Science, Graduate School of Science, Osaka University  
1-1 Machikaneyama, Toyonaka, Osaka 560-0043, Japan  
*E-mail(EM): miyata@ess.sci.osaka-u.ac.jp*

## ABSTRACT

MAXI, Monitor of All-sky X-ray Image, is an X-ray observatory on the international space station. MAXI carries two kinds of slit scanning camera; gas slit camera (GSC) and solid-state slit camera (SSC). In the course of one station orbit, MAXI can scan almost the entire sky with a precision of  $1.5^\circ$  and with an X-ray energy range of 0.5–30 keV. Major purpose of MAXI is monitor of known X-ray sources and detection of new serendipitous sources such as X-ray nova whereas diffuse X-ray emission in our galaxy is also an important target especially for SSC. The good energy resolving power of SSC enables us, for the first time, to map the entire sky with various line emission from O to Fe. Based on the previous observational data, we simulate MAXI data both for SSC and GSC. Large-scale structures in our galaxy such as supernova remnants, radio loop, superbubbles are possible targets for SSC. The Galactic ridge X-ray emission is important target both for GSC and SSC.

KEY WORDS: X-ray — all-sky survey — diffuse source — all-sky line map

## 1. Introduction

Over the past three decades, several X-ray all-sky monitors have been performed (e.g. Holt 1997). The major purpose of X-ray monitor is detection and localization of X-ray sources and monitor of their intensity variation. The high-sensitive soft X-ray survey was performed by Rosat in the 0.1–2.4 keV energy range (Trümper 1983). More than 100,000 sources were cataloged with the Rosat all-sky survey data (Voges et al. 2000). Since Rosat has high sensitivity for diffuse sources, high resolution ( $\sim 12'$ ) X-ray map has been constructed for seven energy bands (Snowden et al. 1995, 1997). They revealed the global structure of diffuse X-ray emission for soft X-ray sky.

## 2. MAXI

MAXI, Monitor of All-sky X-ray Image, is an X-ray observatory on the Japanese experimental module (JEM) exposed facility (EF) on the international space station (Ueno 2009). MAXI is a slit scanning camera which consists of two kinds of X-ray detectors: one is a one-dimensional position-sensitive proportional counter with a total area of  $\sim 5000\text{ cm}^2$ , the Gas Slit Camera (GSC; Mihara et al. 2002), and the other is an X-ray CCD array with a total area of  $\sim 200\text{ cm}^2$ , the Solid-state Slit Camera (SSC; Katayama et al. 2005). GSC subtends a field of view with an angular dimension of  $1.5^\circ \times 160^\circ$  while SSC subtends a field of view with an angular dimension of  $1.5^\circ \times 90^\circ$ . In the course of one station orbit, MAXI can scan almost the entire sky with a precision of

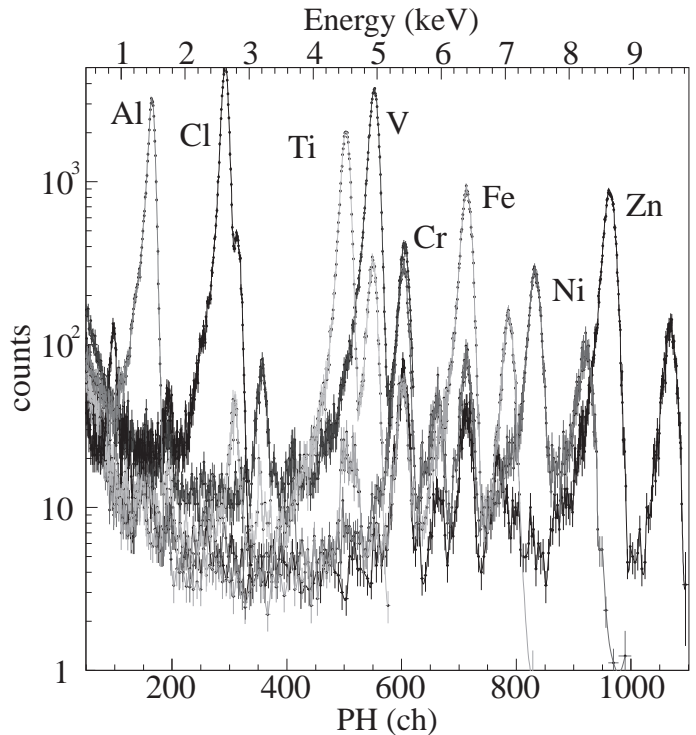


Fig. 1. Histogram of fluorescent X-rays from Al, Cl, Ti, V, Cr, Fe, Ni, and Zn obtained with SSC.

Table 1. Specifications of GSC and SSC.

|                     | GSC   | SSC                   |
|---------------------|---|-----------------------|
| X-ray detector      | 12 units of position-sensitive proportional counter | 32 chips of X-ray CCD |
| Energy range        | 2–30 keV  | 0.5–15 keV            |
| Detector area       | 5350 cm <sup>2</sup>                                | 200 cm <sup>2</sup>   |
| Energy resolution   | 18% at 5.9 keV                                      | 2.5% at 5.9 keV       |
| Field of view       | 1.5°×160°   | 1.5°×90°              |
| Position resolution | 1 mm  | 24 μm                 |

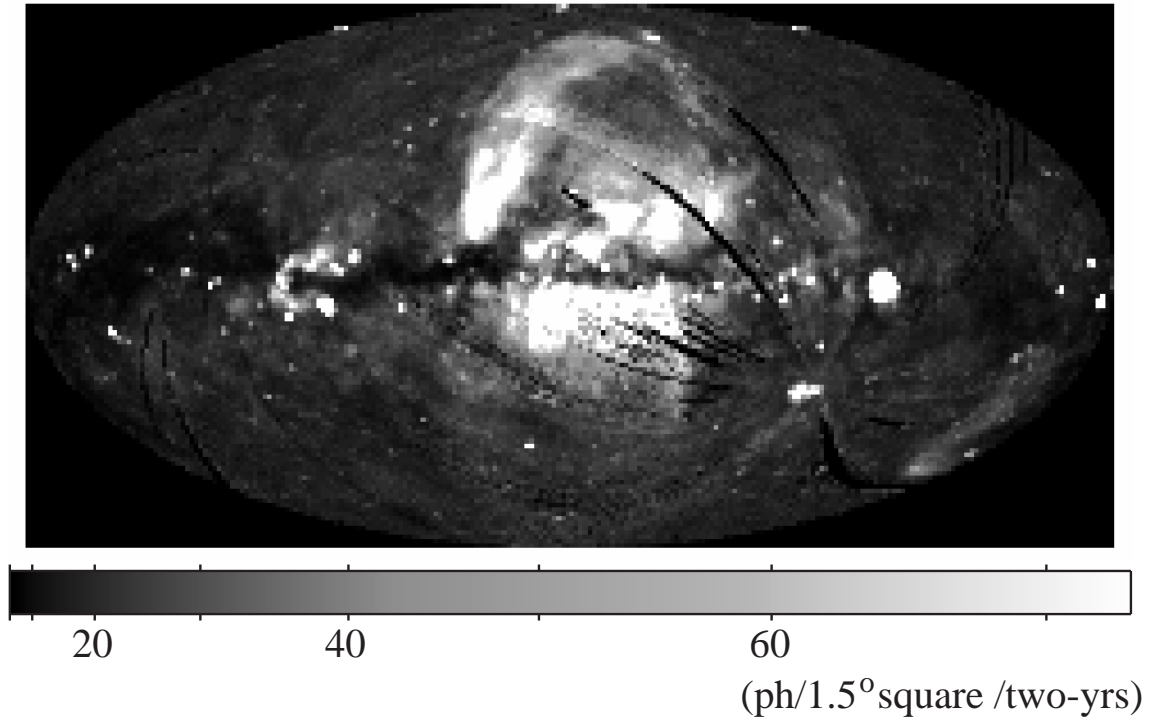


Fig. 2. O line map simulated for the two-yrs observation with SSC.

1.5° and with an X-ray energy range of 0.5–30 keV. Details of both detectors are summarized in Table 1. The mission life of MAXI is two yrs.

The moderate energy resolution of SSC shown in Table 1 enables us to resolve emission lines from heavy elements from O to Fe. Figure 1 shows the histogram of fluorescent X-rays from Al, Cl, Ti, V, Cr, Fe, Ni, and Zn obtained with SSC. Each emission line can be clearly resolved with SSC. SSC possesses the capability to map the entire sky with line emission from O to Fe for the first time. On the other hand, GSC can map the entire sky only with Fe whereas the effective area at Fe line is an order of magnitude larger than that of SSC. Such narrow-band imaging is a powerful tool for the long-term all-sky observation because this technique can be minimized the contamination of the non X-ray background originated in the detector.

### 3. Simulation Data for MAXI

In this section, we demonstrate the data simulated for MAXI.

#### 3.1. O line map

O is one of the most abundant heavy elements in the universe. The full-width at half maximum energy resolution of SSC at O line is  $\sim 80$  eV. This resolution is limited by the relatively warm operating temperature of SSC ( $-50 \sim -60^\circ\text{C}$ ). The separation of He-line O (O VII) and O Ly $\alpha$  is astrophysically important whereas it is difficult with SSC. These emission lines traces warm gas in our galaxy.

Based on the Rosat all-sky survey data, we simulated the O line map with the two-yrs observation of SSC. We employed 3/4 keV data since O line emission is dominant in this energy band. Figure 2 shows the O VII + O Ly $\alpha$  line map simulated for the two-yrs observation with SSC. As clearly demonstrated in this figure, we can expect to map the entire sky only by O lines with high statistics. The brightest object in this band is Puppis-A and the Vela supernova remnant (SNR). The Cygnus Loop is the second brightest object. Other large-scale structures are also possible targets for SSC such as Loop-I, Cygnus superbubble, Orion-Eridanus superbubble. X-ray emission from the Galactic bulge may be a good target.

#### 3.2. Supernova remnants

The brightest target of SSC in the O band is Puppis-A and the Vela SNR. Figure 3 shows the O line map of Puppis-A and Vela SNR simulated for the two-yrs observation with SSC. The large apparent size of the Vela SNR (diameter of  $8.3^\circ$ ; Aschenbach et al. 1995) enables us to study the spatially-resolved spectrum with SSC as shown in Figure 3. Since the Vela SNR is located far from the Galactic plane, the contamination of the Galactic diffuse emission can be negligibly small. This simulated

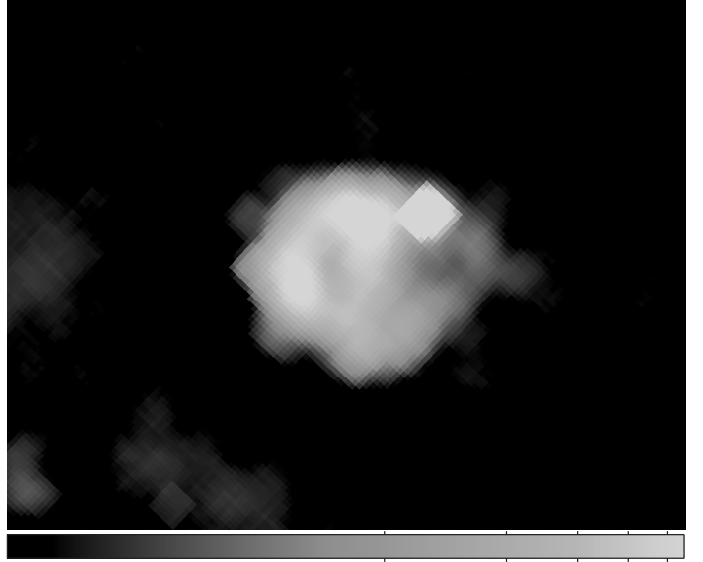


Fig. 3. O line map of Puppis-A and Vela SNR simulated for the two-yrs observation with SSC.

image closely resembles the X-ray surface brightness map of the young SNR Cassiopeia-A observed with the ASCA SIS (Holt et al. 1994). We thus expect good scientific results of the Vela SNR with SSC similar to those of Cassiopeia-A with SIS.

Since the beam size of SSC is  $1.5^\circ$  square, other SNRs are too small for SSC.

#### 3.3. Loop I / North Polar Spur

Loop I is a Galactic giant radio loop of  $58^\circ$  radius centered at  $l=329^\circ$  and  $b=17.5^\circ$  (Egger & Aschenbach 1995). The brightest part of Loop I, in the north-east, has been called the North Polar Spur. The origin of Loop I is still unclear. Previous studies suggested that Loop I is an old, nearby SNR with a non-thermal shell, the remnant of a starburst, or explosion near the Galactic center (Miller et al 2008).

SSC enables us to observe the entire region of Loop I with the CCD resolution for the first time. Based on the spatially-resolved spectral analysis of Loop I, we can study its plasma diagnostics in detail. We can thus calculate the various physical parameters such as abundances of heavy elements, thermal energy, and thermal pressure for the first time. These parameters are clue to investigate the origin of Loop I.

#### 3.4. Superbubbles

As shown in Figure 2, the Cygnus superbubble and the Orion-Eridanus superbubble can be mapped with SSC. Superbubbles are thought to be produced as large hot stars interact with the surrounding interstellar medium. The Cygnus superbubble and the Orion-Eridanus superbubble are large nearby superbubbles created by the

Cygnus OB2 association and the Orion OB1 association, respectively.

SSC enables us to observe the entire region of these superbubbles. Thanks to the good energy resolving power of SSC, we can study the plasma diagnostics and their spatial variation, resulting in the calculation of the total thermal energy and the thermal pressure. These parameters are key to study the evolution of warm and hot gas in our galaxy.

### 3.5. Galactic ridge X-ray emission

The X-ray sky along the Galactic plane exhibits many bright X-ray point sources (e.g. Warwick et al. 1985, 1988). Faint and unresolved X-ray emission is also observed with a half-thickness of 240 pc (Worrall 1982). Highly-ionized iron line (6.7 keV) is detected with the Tenma satellite (Koyama et al. 1986). This line emission together with the continuum emission suggested that the Galactic ridge X-ray emission (GRXE) is thermal radiation from optically thin plasma. So far most of X-ray satellites have spent significant amounts of their observing time to study GRXE, its origin has not yet been elucidated. Whether GRXE is truly diffuse emission or composed of numerous dim point sources remains inconclusive.

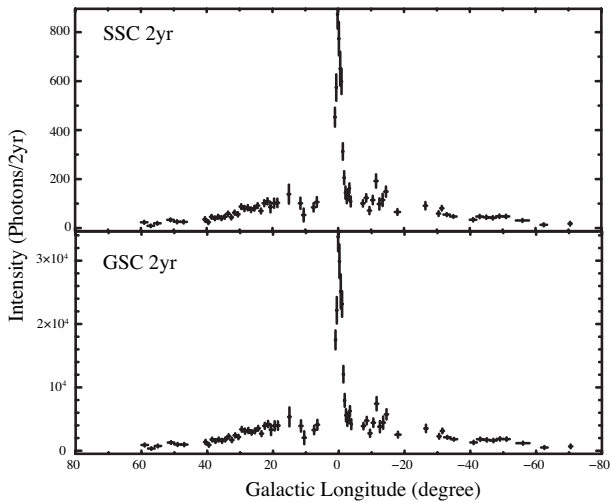


Fig. 4. Intensity profile of 6.7 keV line at the Galactic ridge simulated for GSC and SSC.

Based on the Ginga scanning observation (Yamauchi & Koyama 1993), we simulated the intensity profile of 6.7 keV line at the Galactic ridge for the two-yrs observation both with GSC and SSC, shown in Figure 4. As clearly shown in this figure, we can detect 6.7 keV line with high statistics not only at the Galactic center but also at the Galactic ridge. MAXI furthermore enables us to map the 6.7 keV line at the entire region of the Galactic ridge.

Recent Suzaku observation revealed that Fe line emission consists of three narrow Fe K-emission lines from low-ionized (6.41 keV), He-like (6.67 keV), and H-like (7.00 keV) (Ebisawa et al. 2008). Collisional ionization equilibrium plasma is the likely origin for the 6.67 keV and 7.00 keV lines; however, the origin of the 6.41 keV line, which is due to fluorescence from cold material, has not been elucidated.

With SSC, we can resolve three lines of Fe complex. Based on the Suzaku observational data, we estimated intensities of 6.41 keV, 6.67 keV, and 7.00 keV line to be 26 ph, 119 ph, and 26 ph at typical  $1.5^\circ$  square region for the two-yrs SSC observation, respectively. We can therefore study the spatial variation of these three lines at the Galactic ridge. Spatial variation of line intensity ratio of 6.67 to 7.00 keV allows us to investigate the temperature variation, which gives us an important clue to origin of hot gas; superposition of point sources or diffuse sources.

Origin of 6.41 keV is not also elucidated. Valinia et al. (2000) proposed interactions between the interstellar medium and cosmic supra/non-thermal electrons are responsible for 6.41 keV line. Revnivtsev et al. (2006) proposed that a superposition of numerous, different kinds of point sources may create iron line complex (e.g. cataclysmic variables). In both cases, the spatial variation of 6.41 keV is a key issue. With SSC, we expect 26 ph at  $1.5^\circ$  square region for 6.41 keV line. We can therefore investigate the spatial variation of 6.41 keV line at the entire region of the Galactic ridge. The correlation between 6.41 keV spatial distribution and the spatial distribution of CO or star may give us an important clue to the origin of 6.41 keV line.

It is known that GRXE has low-temperature component with  $kT_e \simeq 0.8$  keV (Kaneda et al. 1997; Ebisawa et al 2005). Highly-ionized emission lines from Ne, Mg, Si, S, Ar, Ca, and Fe-L are detected whereas its origin is also unknown.

Table 2. Intensities of emission lines from various ions for low- $kT_e$  component of GRXE simulated for the two-yrs observation of SSC.

| Emission line | ph/two-yrs/ $1.5^\circ$ square |
|---------------|--------------------------------|
| Fe XVII       | 29                             |
| Ne IX         | 44                             |
| Mg XI         | 48                             |
| Si XIII       | 60                             |
| Si XIV        | 14                             |
| S XV          | 54                             |
| S XVI         | 23                             |
| Ar XVII       | 24                             |

We calculated the intensities of emission lines from various ions for low- $kT_e$  component of GRXE observed

with SSC based on the Suzaku observation (Ebisawa et al. 2008). As shown in Table 2, we can detect various emission lines from the Galactic ridge at typical  $1.5^\circ$  square region with enough statistics to perform the plasma diagnostics. We therefore investigate the spatial structure of low- $kT_e$  plasma. If nonequilibrium ionization condition is confirmed, SNR origin is most likely for low- $kT_e$  component.

#### 4. Conclusion

Major purpose of MAXI is monitor of known X-ray sources and detection of new serendipitous sources such as X-ray nova whereas diffuse X-ray emission in our galaxy is also an important target especially for SSC. The good energy resolving power of SSC enables us, for the first time, to map the entire sky with various line emission from O to Fe. We can study the Galactic large-scale structures such as supernova remnants, radio loop, superbubbles with SSC. The Galactic ridge X-ray emission is the important target both for GSC and SSC. In order to study the diffuse emission, we need to accumulate all X-ray data obtained during the whole mission life. Therefore, stable detector responses over the mission life are essential. We are also required a precise onboard calibration to achieve the good energy resolving power of the detector.

We would like to thank Drs. Ebisawa and Yamauchi for many useful comments and suggestions. EM is supported by Grant-in-Aid for Specially Promoted Research (16002004). Part of this research has made use of data obtained through the High Energy Astrophysics Science Archive Research Center Online Service, provided by the NASA/Goddard Space Flight Center.

#### References

- Aschenbach B. 1995 *Nature*, 373, 587  
Ebisawa K. et al. 2005 *ApJ*, 635, 214  
Ebisawa K. et al. 2008 *PASJ*, 60, S223  
Egger R.J. & Aschenbach B. 1995 *A&A*, 294, L25  
Holt S.S. 1994 *PASJ*, 46, L151  
Holt S.S. 1997 *Proc. All-Sky X-ray Observations in the Next Decade*, 9  
Kaneda, H. et al. 1997 *ApJ*, 491, 638  
Katayama H. 2005 *Nucl. Inst. and Meth. A*, 541, 350  
Koyama K. et al. 1986 *PASJ*, 38, 121  
Mihara T. 2002 *Proc. SPIE*, 173, 186  
Miller E.D. 2008 *PASJ* 60, S95  
Revnivtsev, M. et al. 2006 *A&A*, 452, 169  
Snowden S.L. et al. 1995 *ApJ*, 454, 643  
Snowden S.L. et al. 1997 *ApJ*, 485, 125  
Trümper J. 1983 *Adv. Space Res.*, 2(4), 241  
Ueno S. 2009 in these proceedings  
Valinia A. et al. 2000 *ApJ*, 543, 733

- Voges W. et al. 2000 *IAUC*, 7432  
Worrall D.M. et al. 1982 *ApJ*, 255, 111  
Warwick R.S. et al. 1985 *Nature*, 317, 218  
Warwick R.S. et al. 1988 *MNRAS*, 232, 551  
Yamauchi S. & Koyama K. 1993 *ApJ*, 404, 620